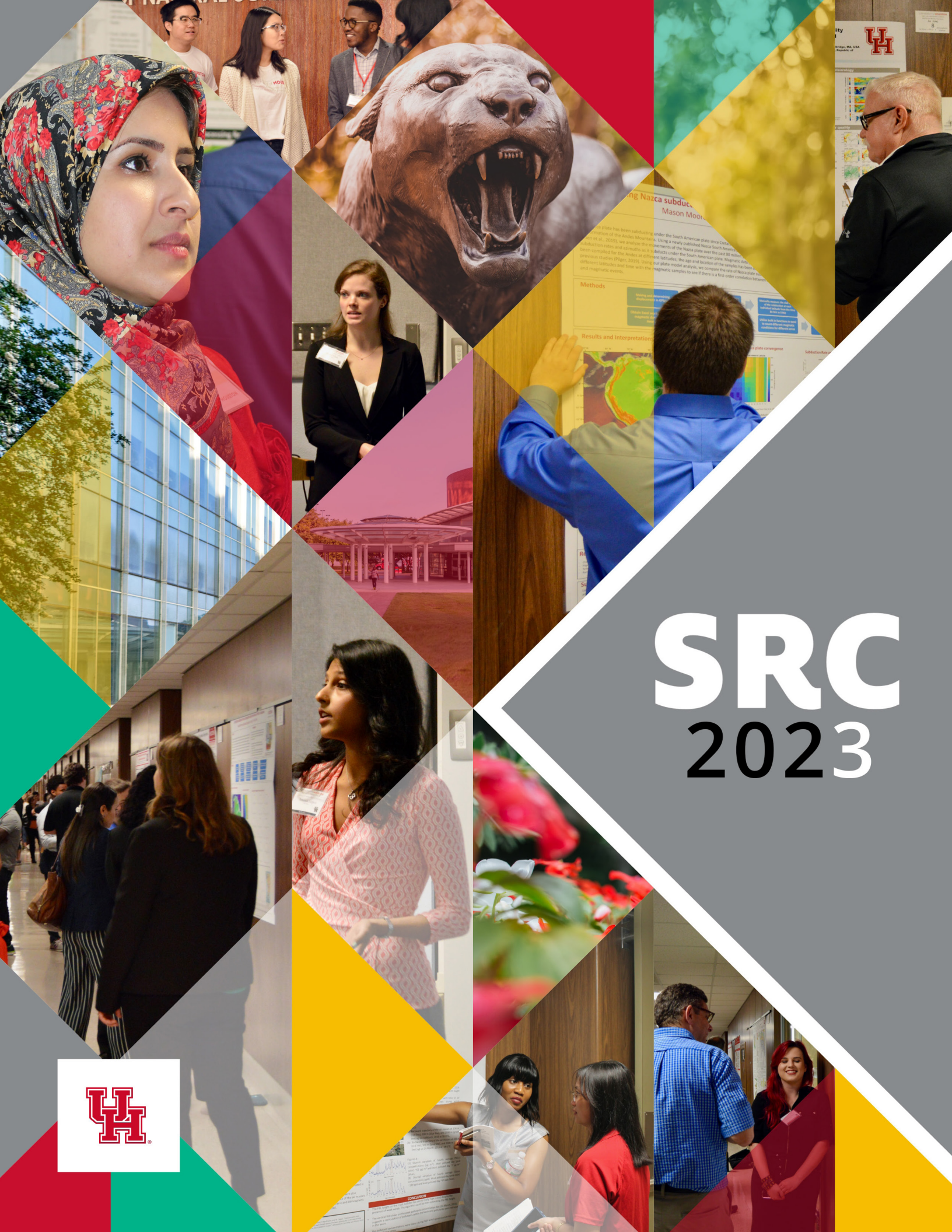

SRC 2023

UNIVERSITY of

HOUSTON

EARTH AND ATMOSPHERIC SCIENCES

36TH ANNUAL

STUDENT RESEARCH CONFERENCE

AND

ALUMNI & INDUSTRY OPEN HOUSE

FRIDAY, APRIL 28, 2023

Table of Contents

American Meteorological Society
UHStudentAMS@gmail.com

AAPG Wildcatters
AAPG.Wildcatters@gmail.com

GeoSociety
GeoSocietyatUH@gmail.com

SEG Wavelets
SEGWavelets@gmail.com

AEG & AIPG
AEGatUH@gmail.com

Schedule
& Logisctics

Check-in | Registration	**8:30 - 9:00 am**
Oral Presentations	**9:00 - 10:30 am**
Coffee Break	**10:30 - 11:00 am**
Oral Presentations	**11:00 - 12:30**
Lunch Break	**12:30 - 1:00 pm**
Poster Presentations	**1:00 - 2:45 pm**
Keynote Speech	**3:00 - 3:30 pm**
Awards Ceremony	**3:30 - 4:30 pm**
Group Photo	**4:30 pm**
Happy Hour	**5:00 - 7:30 pm**

Judges Room
SR1 Rm 130

Orals
Advanced Ph.D.:
SR1 Rm 634
Starting at 9:00 am

MS and 1st year Ph.D.:
SR1 Rm 223
Starting at 9:30 am

Undergraduate:
SR1 Rm 410
Starting at 11:00 am

Posters
All Students:
SR1 2nd Floor

Keynote speech | Awards ceremony
SR1 Rm 116

Advance Phd Oral Presentations

9:00 AM

Morshad Ahmed

Source apportionment of gaseous Nitrophenols and their contribution to HONO formation in an urban area

9:15 AM

Claudia Bernier

Evaluating 3-D ozone observations using an air quality model during the TRACER-AQ campaign in Houston, TX

9:30 AM

Boming Wu

Convolutional Neural Network-assisted least-squares migration

10:00 AM

Travis Griggs

Characterizing Over Water High Ozone Events in the Houston-Galveston-Brazoria Region During the 2021 GO3 and TRACER-AQ Field Campaigns

10:15 AM

Michael Comas

Sedimentary Record of Recent Retreat of Pine Island Glacier, Amundsen Sea, Antarctica

11:00 AM

Semko (Mahmoudreza) Momeni

Developing a python-based data assimilation framework (pyDAF) to Refine Estimates of Emissions

11:15 AM

Kamil Qureshi

Surface Deformation of the Western Himalayan Frontal Thrust System: An insight from InSAR Time-series Analysis.

11:30 AM

Tanzina Akther Akther

Volatile Organic Compounds (VOCs) Source Identification in Mexico City and Future Study of VOC Surface Emission using 2DGC

12:00 AM

Juan Pablo Ramos Vargas

Crustal structure of the Colombian basin and significance for Caribbean tectonic history and its hydrocarbon potential

12:15 AM

Hadi Zanganeh Kia

Large Eddy Simulation of sneeze plumes and particles in a poorly ventilated outdoor air condition: A case study of the University of Houston main campus

MS/ Early Ph.D Presentations

9:30 AM

Julia Villafranca

Sediment Deposition as a Function of Holocene Glacier Retreat, Amundsen Sea, Antarctica

9:45 AM

Sharmila Appini

Intra-slab anisotropy beneath Japan through Shear Wave Splitting

10:00 AM

Karissa Vermillion

The importance of the San Gabriel Mountains to the tectonic reconfiguration of southern California

10:15 AM

Sai Udaya Meghana Yella

A Study on Helium

11:00 AM

Basil Onyekayahweh Nwafor

Unravelling the evolution and characteristics of Tertiary intertidal environment using Broadband seismic and biostratigraphic data: an evaluation of offshore Malay Basin

11:15 AM

Nima Khorshidian

Cloud Formation and Precipitation over Texas: Improving Model Simulations using Observation Nudging and Detailed Microphysics

11:30 AM

Md Upal Shahriar

Defining the crustal structure of the rifted-passive margin of Mauritania and implications for its hydrocarbon potential

Undergraduate Presentations

11:00 AM

Faith Walton

Structural restoration and driving forces for the Oligocene-Recent opening of the Gulf of California

11:15 AM

Jason Ruszkowski

Sampling Microplastics and Extremophile on Balloon Borne Payloads

11:30 AM

Borna Koohbor

The Impacts of Temperature and Humidity on the Light Scattering Properties of Sulfur-derived and Calcite Aerosols

12:00 AM

Aliasghar Shariff

Auroral Spectroscopy

12:30 AM

Celine Saidy

Gaseous Compounds: Measuring the Composition of Trace Gasses in Earth's Atmosphere

Graduate Poster Presentations

2-1A	Lisabeth Arellano
2-2A	Larkin Spires
2-3A	Irfan Karim
2-4A	Jincheol Park
2-5A	Moloud Rahimzadeh
2-6A	Divin Kalu
2-7A	Sara Rojas
2-8A	Kenneth Shipper
2-22A	Nina Zamanialavijeh
2-9F	Xinyue Wang
2-10F	Mayra Lopez Carrasquilla
2-11F	Madison Rafter
2-12F	Mahsa Payami
2-13F	Ronin Costello
2-14F	Geoffrey Roberts

Undergraduate Poster Presentations

2-15U	Noelle Cheshire
2-16U	Emily Stivison
2-17U	Nynaeve Phillipson
2-19U	Joseph McNease
2-20U	Leo Collier
2-21U	Johanna Villagomez

Dr. James Flynn

KEYNOTE SPEAKER

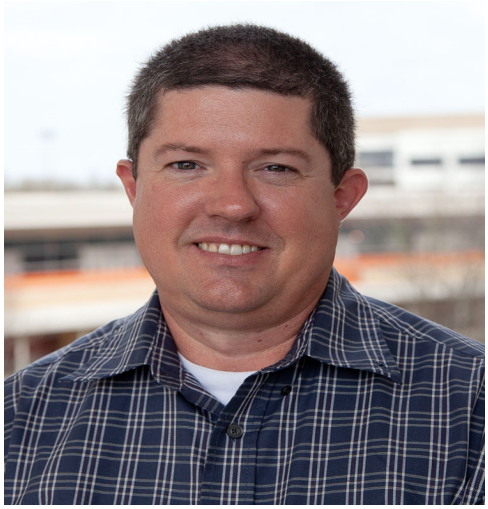

Dr. James Flynn is a Research Associate Professor in the Department of Earth & Atmospherics Sciences at the University of Houston. He has been recently named a Senior Member of the National Academy of Inventors (NAI). Dr. Flynn got his Ph.D. in 2013 from UH in Atmospheric Sciences with a specialization in Atmospheric Chemistry.

"Preliminary results from recent Houston air quality studies and what comes next"

Lab Open House

ICP Research Lab

Location: SR1, Room 332 and Room 334

The ICP (Inductively Coupled Plasma) Research Laboratory and Agilent Facility Center in the Department of Earth & Atmospheric Sciences specializes in characterizing the chemical and isotopic compositions of materials, including the ability to provide in-situ micron scale analyses of solid samples with the state-of-art Laser Ablation System.

Faculty host: Yongjun Gao, Minako Righter, John F. Casey
Web site: http://icplab.geosc.uh.edu/

GCxGC/MS Facility for Multidisciplinary Applications

Location: SR1, Room 430

This lab has a Shimadzu GCxGC/MS system coupled to a Zoex modulator which is capable to analyse complex matrices of volatile organi`c compounds (VOCs). The system is complemented by a PICARRO G2201-i CRDS (cavity-ring-down spectrometer) instrument to measure methane (CH4) and carbon dioxide (CO2) along with their 13C and 12C isotopes to distinguish among different carbon pools. For offline sampling the lab uses stainless steel canisters and adsorption tubes depending on the target analytes. Current research interest addresses unconventional sources for reactive organic carbon (ROC), per- and polyfluoroalkyl substances (PFAS) and phthalates. The lab is open to serve internal and external users in the field of atmospheric composition, emission sources, energy transformation, exposure studies and medical sciences.

Faculty host: Bernhard Rappenglueck
Web site: https://icas.uh.edu

Rock Physics Lab (RPL)

Location: SR1, Room 104-108, B-8

Rock Physics Lab (RPL) is a research lab to conduct world class research on Seismic Rock Physics. Based on our 25+ years' experiments and achievements on seismic rock physics and collaboration with industry through the Fluids/DHI Consortium, we have been focusing on energy transition, especially on GCS and geothermal. From lab data measurement, model development, to application software, we use integrated research strategies of combining the fluid and rock properties to provide academic results and industry solutions. The lab research focuses on:

1. Seismic properties of hydrocarbon fluids at in-situ conditions and rocks from conventional reservoirs (sands, sandstone, tight gas sands and carbonates);
3. All kinds of rocks and fluids from unconventional reservoirs: oil shale, shale gas, shale oil, coal, gas hydrate, and heavy oil sands;
4. Rock parameters, seismic velocities, modulus, including rock mechanics and LF measurements;
5. Experimental and theoretical investigation on poro-elasticity (including digital rock modeling), velocity dispersion, wave attenuation, elastic anisotropy, fractured reservoir, static and dynamic elasticity;
6. Seismic attributes as direct hydrocarbon indicator (DHI), reservoir delineation, 4-D seismic monitoring, manage unconventional reservoirs;
7. Physical and seismic properties of rocks and fluids related to energy transitions: GCS and geothermal;
8. Training graduate students.

Faculty Host: Dr. Yingcai Zheng and Dr. De-hua Han
Website: http://www.rpl.uh.edu/

The laser ablation MC-ICP-MS lab

Location: SR1 Room 317

The Multi-Collector ICP-MS (Inductively Coupled Plasma) lab is capable of analyzing a wide range of geochronologic isotope systems including samarium-neodymium and lutetium-hafnium dating of igneous and metamorphic rocks as well as stable isotope systems such as lithium, magnesium, silicon, iron, and mercury.

We are equipt with a class 500 metal-free clean laboratory for sample preparation prior to inorganic elemental and/or isotopic analysis. In-situ U-Th-Pb dating as well as in-situ minor and trace element analyses can be done using the Photon Machine Excite laser ablation system coupled with the Plasma Quant Elite ICP-MS.

Faculty host: Thomas Lapen, Minako Righter, Yongjun Gao

Advanced PhD Oral Presentations

Boming Wu

Convolutional Neural Network-Assisted Least-Squares Migration

Least-squares migration (LSM) is a data-fitting imaging approach seeking the seismic reflectivity image of the most accurate amplitude and optimal resolution. However, the high computational cost of LSM has hindered its broad application. In this study, we combine a convolutional neural network (CNN) with LSM to significantly improve computational efficiency while retaining imaging quality. Taking CNN as a "projector", we treat LSM as the "projection" from the ordinarily migrated images to the least-squares updated images. We conduct this CNN-assisted LSM in the shot gather domain using a Gaussian beam migration and the corresponding LSM. The training data for CNN consists of 10-15% of all shot gathers, with the Gaussian beam migrated shot gathers as the input, and the LSM shot gathers as the target. After the training, the processing time for the remaining shot gathers took several minutes for 2D cases. The results from testing with the Sigsbee2B synthetic dataset and a field marine dataset indicate the CNN-assisted LSM saved 80-90% of the computation time of the full LSM, and achieved significantly higher image fidelity than that of the ordinary migration

Claudia Bernier

Evaluating 3-D ozone observations using an air quality model during the TRACER-AQ campaign in Houston, TX

The Houston-Galveston-Brazoria (HGB) region is susceptible to unique local emissions, transport, and meteorological factors that lead to large tropospheric ozone variations. A consistent and highly detailed variety of measurements is essential in understanding the development and behavior of tropospheric ozone in this region. The 2021 Tracking Aerosol Convection ExpeRiment – Air Quality (TRACER-AQ) campaign addressed this need by utilizing ozone lidars, sondes, off-shore boats, aircraft, and a string of additional measurements to capture a wide range of ozone cases in the HGB region for the month of September. Using the multi-dimensional ozone lidar curtain profile observations, we investigate diverse vertical and temporal fine tropospheric ozone cases. The WRF-Chem model is run for the course of the campaign period at 1.33 km to evaluate the performance of high-resolution temporal and vertical ozone simulations.

Hadi Zanganeh Kia

Large Eddy Simulation of sneeze plumes and particles in a poorly ventilated outdoor air condition: A case study of the University of Houston main campus

Since the outbreak of the COVID-19 pandemic, many previous studies using computational fluid dynamics (CFD) have focused on the dynamics of air masses, which are believed to be the carriers of respiratory diseases, in enclosed indoor environments. Although outdoor air may seem to provide smaller exposure risks, it may not necessarily offer adequate ventilation that varies with different micro-climate settings. To comprehensively assess the fluid dynamics taking place in outdoor environments as well as the efficiency of outdoor ventilation, we simulated the outdoor transmission of a sneeze plume in "hot spots," or areas in which the air is not quickly ventilated. We began by simulating the airflow over buildings at the University of Houston using an OpenFOAM computational fluid dynamics solver that utilized the 2019 seasonal atmospheric velocity profile from an on-site station. Next, we calculated the length of time that an existing fluid resides in the domain by defining a new variable and then selected the hot spots. Finally, we conducted a large-eddy simulation of a sneeze in outdoor conditions and then simulated a sneeze plume and particles in a hot spot. The results show that it takes as long as 1,000 seconds for fresh incoming air to ventilate the hot spot area in some specific regions on campus. We also found that even the smallest amount of upward wind causes a sneeze plume to dissipate almost instantaneously at lower elevations. However, downward wind provides a stable condition for the plume, and forward wind can carry a plume even beyond six feet, the recommended social distance for preventing infection. Additionally, the simulation of sneeze droplets shows that the majority of the particles adhered to the ground or body immediately, and airborne particles can be transported more than six feet, even in a very small amount of ambient air.

Juan Pablo Ramos Vargas

Crustal structure of the Colombian basin and significance for Caribbean tectonic history and its hydrocarbon potential

Two previous hypotheses have been proposed to explain the crustal types underlying the 3-4-km deep waters of the Colombian basin on the southwestern margin of the Caribbean: 1) an area of older, normal thickness oceanic crust of Cretaceous to Jurassic age in the eastern Pacific Ocean was partially covered by the Caribbean large igneous province (CLIP) inferred to have formed as a 15-20- km-thick oceanic plateau related to the Galapagos hotspot during the period from Cenomanian to Coniacian (95-88 Ma); and 2) small areas of normal thickness oceanic crust of Miocene age rifted apart the older and thicker CLIP. I test both hypotheses by interpreting a grid of 8000 km of 2D seismic reflection data, a grid of 13,000 km2 of 3D seismic reflection data; magnetic and gravity data, vintage refraction data, and a compilation of DSDP, ODP, and industry wells. Detailed stratigraphic correlations support the first hypothesis of the older, oceanic crust overlain by the younger CLIP. The various data sets allow me to precisely define the boundaries of the older oceanic crust which a previous study of magnetic anomalies proposes having formed in the Late Cretaceous along with a WNW-striking extinct spreading ridge and orthogonal transform fault. I use a Gplates model to show how this area of Cretaceous oceanic crust formed in a slow-spreading environment of the Eastern Pacific Ocean and was transported eastward into the Caribbean region. Sedimentary isopach maps show the thickening of the late Cretaceous section along the extinct and elongated ridge and transform along with troughs formed parallel to the adjacent abyssal hills topography. This late Cretaceous section can be correlated with high TOC rocks of Coniacian to Santonian age recovered from DSDP sites on the elevated Beata Ridge adjacent to the Colombian basin. Gas chimneys emanating from the equivalent late Cretaceous interval buried by a 10-km-thick clastic overburden of the Magdalena deepsea fan, the presence of oil seeps, and biomarkers recovered from piston core samples indicate the thermal maturity of these source rocks over a widespread area of the deepwater Colombian basin.

Kamil A. Qureshi

Surface Deformation of the Western Himalayan Frontal Thrust System: An insight from InSAR Time-series Analysis.

Most of the present-day stresses associated with the India-Eurasian convergence are accommodated by the Main Frontal Thrust (MFT) in the form of seismic and aseismic creep. However, the amount of surface deformation associated with MFT is poorly constrained. This study investigates the surface deformation associated with frontal thrusts known as Salt and Trans Indus Ranges at the western margin of the Indian plate. We have employed short baseline subset (SBAS) Interferometric Synthetic Aperture Radar (InSAR) technique. The temporal coverage spans from Feb 2017 to June 2022 and utilized both ascending and descending track geometry of Sentinel-1A mission. The satellite line of sight displacement map shows active deformation associated with Kalabagh Fault, Pezu Fault, and Kurram Fault. The InSAR time-series show ~ 6 mm/year deformation of Kalabagh Fault, ~ 5.5 mm/year of Pezu thrust, and ~ 2 mm/year for Kurram Fault, respectively. The Kurram Fault shows both seismic and aseismic creep along the length of its segment, which is shown both from satellite line of sight displacement map and seismic events. While Kalabagh Fault and western Salt Range shows aseismic creep during the investigated time-period due to the presence of ductile Precambrian Salt Range Formation. Hence, this study provides a detailed surface displacement map and associated potential seismic hazards.

Michael Comas

Sedimentary Record of Recent Retreat of Pine Island Glacier, Amundsen Sea, Antarctica

The meltwater volume from Pine Island Glacier (PIG) has been recently identified as the single-largest contributor to global sea-level rise from all of Antarctica. The destabilization of PIG, and other glaciers terminating in the Amundsen Sea Embayment (ASE), has been tied to changes in climate over the Southern Ocean. Oceanographic sampling in, and models of, the ASE have found that slightly warmer Circumpolar Deep Water (CDW) has been advecting onto the continental shelf as a response to strengthening winds in the region. The continental shelf in West Antarctica has a reverse-sloping bed topography which was carved after repeating cycles of glaciation, and provides avenues for the denser CDW to travel down-slope and reach the grounding line of ASE glaciers. The exact timing of the first incursions of CDW onto the shelf of the ASE is unknown; however, since the beginning of satellite data acquisition over West Antarctica, PIG has been experiencing ice shelf thinning and grounding line retreat. Studies have already been conducted to broadly characterize the path and style of West Antarctic Ice Sheet retreat through the ASE since the last glacial maximum, but little work has done to understand why and how the retreat of PIG (and other glaciers) has been recently reinitiated. This study seeks to provide a detailed understanding of PIG's pre-satellite dynamics by investigating properties of sediments collected proximal to PIG. Sediments cores were collected in 2020 aboard the RV/IB Nathaniel B. Palmer from an area of newly-exposed seafloor immediately following the calving of a large portion of Pine Island Ice Shelf. Initial core descriptions and analysis suggest that the retreat of PIG's grounding line has been preserved where very poorly sorted diamicts (sub-glacial deposits) are overlain by finer-grained, well-sorted sediment drapes (glacial-marine deposits). To determine the timing of these changes in environment at each core site, grainsize and grain-shape analysis will be conducted alongside radio-isotopic dating methods. Measurements of excess 210Pb activity within the seafloor sediments and 14C from foraminiferal tests allow for the construction of age models to establish timing and rates of sediment deposition in the area. Determining the timing and pace of PIG's modern retreat will aid in the constraining of models of the glacier's dynamics which is a crucial step in preparing for global sea-level rise in the near future.

Morshad Ahmed

Source apportionment of gaseous Nitrophenols and their contribution to HONO formation in an urban area

Nitrophenols (NPs) are compounds that comprise of hydroxyl- and nitro- functional groups attached to at least one aromatic ring. Nitrophenols (NPs) have significant impacts on human health, climate, and atmospheric chemistry. Despite numerous measurements of particle NPs, still little is known about their atmospheric abundances, sources, and fate. Here, four gaseous NPs [2,4-dinitrophenol (2,4-DNP), 4-nitrophenol (4-NP), 2-nitrophenol (2-NP), and 2-Methyl-4-nitrophenol (2-Me-4-NP)] were continuously monitored during late Spring at an urban site in Houston, Texas. Among the four NPs, 4-NP showed the highest abundance, followed by 2-Me-4-NP, 2-NP, and 2,4-DNP with average concentrations of 0.47 ± 0.12 ppt, 0.41 ± 0.16 ppt, and 0.27 ± 0.09 ppt, respectively. The positive matrix factorization (PMF) model identified seven sources: industrial NPs, secondary formation, phenol sources, acetonitrile source, natural gas/crude oil, traffic, and petrochemical industries/oil refineries. A zero-dimensional photochemical box model was used to simulate the observed 2-NP and 2,4-DNP. A 50.0% and 70.0% JNO2 was found to be consistent with the measured 2-NP and 2,4-DNP. This yields a nitrous acid (HONO) production of 7.5 ± 2.5 ppt/h from 06:00 to 18:00 Central Standard Time (CST) from both NPs. An extrapolation including other known NPs suggests a maximum HONO formation of 11.5 ppt/h. The results of this study suggest that using PMF analysis supplemented by photochemical box model provides identification of the NPs sources and their atmospheric implication to HONO formation.

Semko (Mahmoudreza) Momeni

Developing a python-based data assimilation framework (pyDAF) to Refine Estimates of Emissions

Uncertainties in the input variables of atmospheric models are propagated into their results and degrade the ability of their predictions, which are used to estimate health effects and the uncertainty have negative impact on health estimations. In order to reduce the uncertainties, models can be constrained with observations as the optimal combination of the observed and modeled information can be utilized. Data assimilation technique combines observations and models in a way that accounts for the uncertainties in each while simultaneously respecting certain constraints. Since data assimilation is a powerful tool that has been widely used in investigating the atmosphere and there is no a comprehensive framework to use it, a data assimilation framework that can handle different approaches is of interest. We are developing a python-based data assimilation framework (pyDAF) focusing on 4D-Var in order to refine the estimation of air pollutant emissions through a combination of air quality model and observations. For case study, we are constraining Ammonia (NH3) concentrations to refine NH3 emissions with a combination of observations from satellite-based instrument (Cross-track Infrared Sounder (CrIS)) and chemical transport model with its adjoint (CMAQ adjoint) over East Asia. Noting that NH3 plays a significant role in forming fine inorganic particulate matter (PM2.5) in the atmosphere, which is associated with premature mortality. We first tested the validity of the adjoint-based sensitivities of concentrations with respect to emissions by comparing them to sensitivities calculated with the forward model using the finite difference method. Once confirmed, inorganic PM2.5 and ammonia were simulated over East Asia using the chemical transport model. Then, the influences of emissions on a cost function are determined by using the and the adjoint of model. These spatially-specific sensitivities are evaluated in different regions over the East Asia. Finally, the model adjoint is integrated in the four-dimensional variational data assimilation implemented in pyDAF for future refinement of ammonia emissions over the East Asia.

Tanzina Akther Akther

Volatile Organic Compounds (VOCs) Source Identification in Mexico City and Future Study of VOC Surface Emission using 2DGC

Volatile organic compounds (VOCs) data in conjunction with other inorganic pollutants, surface meteorological data and continuous measurement of the Planetary Boundary Layer height (PBLH) at an urban site in Mexico City were performed from 6 to 18 March 2016 to study ozone formation processes in that city. One aspect also included the analysis of potential emissions sources of ozone precursors. Here, we applied Positive Matrix Factorization (PMF) for emission source identification. The pollutant data base included a large suite of VOCs along with equivalent black carbon (eBC), gaseous pollutants (CO, NO, NO2, SO2, NH3) and ions (Na+, Mg2+, Ca2+, NO3-, NH4+). To some extent the results show emission source factors which can be usually found in urban areas among them evaporation, non-LPG (liquefied petroleum gas) combustion and vehicle exhaust. However, the inclusion of ions in our PMF analyses also allowed to resolve other factors which included secondary aerosol precursors and most interestingly geogenic sources. This presentation highlights potential reasons for these geogenic sources. It also discusses future work to investigate VOCs emissions from unconventional sources, determine source specific VOC fingerprints and evaluate their impact on air quality. Conventional separation techniques cannot resolve the bulk of it, which is commonly called the unresolved complex mixture (UCM). In this work a GCxGC/MS system will be used to quantify both the resolved and unresolved constituents.

Travis Griggs

Characterizing Over Water High Ozone Events in the Houston-Galveston-Brazoria Region During the 2021 GO3 and TRACER-AQ Field Campaigns

Photochemical modeling outputs showing high ozone concentrations over the Gulf of Mexico and Galveston Bay during ozone episodes in the Houston-Galveston-Brazoria (HGB) region have not been previously verified using in-situ observations. Such data, however, was collected from July-October 2021 from three boats deployed for the Galveston Offshore Ozone Observations (GO3) and Tracking Aerosol Convection Interactions ExpeRiment - Air Quality (TRACER-AQ) field campaigns. Specifically, a pontoon boat owned by the University of Houston and a commercial shrimping boat operated in Galveston Bay, and a 30 m commercial service vessel (Red Eagle) operated in the Gulf of Mexico offshore of Galveston. All three boats were instrumented with continuously operating sampling systems that included ozone analyzers and weather stations, with the pontoon and shrimp boat also equipped with a ceilometer. Sampling systems operated autonomously on the shrimp and commercial boats as they traveled along their daily routes. Additionally, 35 ozonesondes were launched on forecasted high ozone days from the pontoon boat in Galveston Bay and the Red Eagle in the offshore waters of the Gulf of Mexico. Multiple periods of ozone exceeding 100 ppbv were observed over water in Galveston Bay and the Gulf of Mexico. These events included previously identified conditions for high ozone events in the HGB region, such as the land-bay-sea breeze circulation and post-frontal environments, as well as a localized coastal high ozone event after the passing of a tropical system (Hurricane Nicholas) that was not well forecast.

MS and 1st year PhD Oral Presentations

Basil Onyekayahweh Nwafor

Unravelling the evolution and characteristics of Tertiary intertidal environment using Broadband seismic and biostratigraphic data: an evaluation of offshore Malay Basin

Analysis of depositional facies using well data plays an important role in the assessment of reservoir quality. However, well datasets are only available after a seismic survey showed potential targets to drill. Though limited resolution could lead to overlooked thin stratigraphic targets, a plausible technique to solve the problem of sole dependency of the depositional model on well data is by incorporating seismic facies analysis. Improving the bandwidth of seismic data is beneficial for the interpretation of thin-layer targets in the workflow for reservoir characterization. Instead of randomly inventing frequencies in this research, we used spectral harmonic extrapolation techniques to obtain broadband seismic data. This technique improves the resolution of the seismic data without boosting unwanted signals. Applying this increased the seismic bandwidth from 80 to 180 Hertz. The enhanced seismic was in turn spectrally decomposed into 25, 35, and 45 Hertz frequency volumes using the generalized spectral decomposition (GSD) algorithm. The GSD is applied to unveil the stratigraphic details contained in the zone of interest because well-resolved reflections from the top and bottom of subtle stratigraphic boundaries can only be seen in thick features imaged with broadband data. The resultant frequency volumes, complemented by biostratigraphic records of four wells, aided the interpretation of stratigraphic records and reconstruction of the depositional history for the Group B stratigraphic sequence in the Northern Malay Basin, Malaysia. Results showed how the sequence evolved from an isolated coastal plain lagoon setting through an intertidal to a fluvial-dominated depositional setting. The spectral broadening of the seismic bandwidth enabled us to enhance the interpretation of complex depositional systems and aided a detailed characterization of such depositional environments using geologically sound constraints.

Julia Villafranca

Sediment Deposition as a Function of Holocene Glacier Retreat, Amundsen Sea, Antarctica

Retreat of ice sheets in Antarctica since the Last Glacial Maximum (LGM) has influenced sediment deposits in the surrounding seas. The West Antarctic Ice Sheet (WAIS), specifically, has experienced rapid retreat due to the characteristic grounding line occurrence below sea-level. High-resolution subbottom seismic data (chirp) collected throughout the Amundsen Sea of West Antarctica reveal sediment deposits influenced by two major glaciers that drain into a major bay of the Amundsen Sea. Thwaites Glacier and Pine Island Glacier have been experiencing not only high ice flow velocity, but an increase in the velocity. This significance causes extreme interest in the subglacial processes, including sediment deposition contributors and controls, occurring in this area characterized by high relief bathymetry. Subbottom profile interpretation of open marine, distal, and proximal ice sheet settings across the Amundsen Sea will be conducted to analyze the relationship of sediment deposits with the morphology of the seafloor. During the austral summer of 2019 and 2020 two research expeditions aimed to collect data from Thwaites and Pine Island Glaciers, respectively, continuously collected chirp profiles across a ~10,000 km track line in the Amundsen Sea using a hull-mounted Knudsen. Past subbottom analysis of this area has not been extensive. In this study, sediment deposits interpreted from the Amundsen Sea chirp profiles will be geometrically characterized as draped, ponded, or chaotic. Draped sediment will follow the morphology of the seafloor and correlates to widespread, low energy, hemipelagic deposition. Ponded sediment will have parallel laminations in seafloor lows and can correlate to episodic or slope related deposition, as well as hemipelagic deposition. Chaotic or reflection free seafloor profiles could be indicative of bedrock and will display a lack of reflectors in a pronounced geometric configuration. These seismic facies will then be mapped across the study area, as well as measured relative vertical thickness. Combined, these analyses can support the further interpretation of depositional controls and processes of the Amundsen Sea, driven by glacial retreat since the LGM.

Karissa Vermillion

The importance of the San Gabriel Mountains to the tectonic reconfiguration of southern California

The San Andreas fault system (SAFS) in southern California is one of the most well-studied plate margins, yet much debate remains on its paleotectonic history. The SAFS was first initiated around ca. 30 Ma because of a fundamental tectonic re-arrangement of southern California. Its subsequent activity has significantly shaped the tectonic history and geography of California. Southern California is a critical component in paleotectonic models for: (1) the evolution of the USA-Mexico Cordillera, (2) the interaction of continental and oceanic plates, and (3) relations between subduction and transform processes during the Mesozoic and Cenozoic. Here, the East Pacific Rise subducted underneath the North American plate just after 30 Ma, leading to complex capture of microplates and development of the SAFS system. After subduction, two triple junctions migrated north and south away from one another, and the plate margin underwent regional extension, transrotation, and transtension prior to formation of through-going strike-slip faults. However, the timing of extension is quite broad (28 to 18 Ma) and the role of extensional structures in partitioning stress as the plate margin developed is unclear. Extensional structures directly related to the paleotectonic history of SAFS are difficult to study because of later deformation, separation, and erosion, but however, are preserved in the San Gabriel Mountains.The Sierra Pelona and Blue Ridge localities of the San Gabriel Mountains host segments of the Chocolate Mountains Anticlinorium (CMA) and coeval sedimentary units. Recent studies concluded that this structure was not only active at ca. 25 – 18 Ma but was already a substantial regional topographic high at 25 Ma, suggesting that extension was ongoing prior. CMA growth may have continued until 9 Ma at Blue Ridge. If a substantial portion of CMA bedrock was removed between 18 – 9 Ma, then the CMA was active between ca. 25 – 9 Ma, with a minimum duration of 16 m.y. This outcome implies that the CMA accommodated substantial strain and was a critical structure during evolution of the SAFS. A better understanding of the tectonic history of the CMA, related extensional structures, and associated sedimentary deposits are critical in understanding the transition from shallow subduction to strike-slip faulting, and the role of low angle extension in abetting the transition.

Md Upal Shahriar

Defining the crustal structure of the rifted-passive margin of Mauritania and implications for its hydrocarbon potential

I have interpreted a grid of 16047.25 line-km of seismic reflection data, various filters of regional gravity and magnetic maps, four previously published refraction lines, and a compilation of DSDP and industry wells in the shelf, slope, and deep basin to define the crustal structure and overlying stratigraphy of the rifted-passive margin of Mauritania and describe how this crustal structure controls its hydrocarbon potential. This integration of these various data types reveals the locations and boundaries of the following tectonic elements: 1) un-extended and full-thickness (30-45 km) continental crust of the West African craton; a map to the top of Paleozoic and older basement and constrained by both well and seismic reflection data shows the lack of rifting across the land area of Mauritania; 2) a relatively narrow (50-150 km) necked zone of rifted continental crust that underlies the coastal area, shelf, and slope of Mauritania; a single large rift with a width of 20-80 km and a continuous, margin-parallel length of 1200 km underlies the shelf and slope of Mauritania and is marked by a prominent zone of salt diapirism; regional seismic lines along the margin show the abrupt transition between the non-volcanic margin in Mauritania with the localized volcanic margin on the Guinea Plateau that has been related to a localized, Jurassic-Cretaceous hotspot track; 3) the continent-ocean boundary between thinned continental crust and Jurassic oceanic crust is mapped from various gravity and magnetic filers but is less well displayed on seismic reflection as a result of its deep burial; and 4) the area of Jurassic oceanic crust includes the thickened area of the Miocene to Recent Cape Verde hotspot; outside the hotspot-affected area, the magnetic expression of the Jurassic oceanic crust is typical of the Jurassic magnetic quiet zone as seen around the margins of the Central Atlantic Ocean; and the oceanic crust is strongly flexed beneath the margin as seen along the Moroccan margin of northwestern Africa; and 4) the stratigraphy of the overlying, Jurassic-Recent passive margin passes from a steep-sided, Jurassic-early Cretaceous carbonate margin that transitions to five overlying, late Cretaceous submarine fans linked to major drainage systems in west Africa; major unconformities within the passive margin section include the Central Atlantic breakup unconformity at its base, the Neocomian unconformity within the carbonate platform, the Albian unconformity marking the Equatorial Atlantic opening to the south and the transition from carbonate to clastic-dominated passive margin, and the Oligocene unconformity marking the eustatic lowstand. Based on this above information, I review various hydrocarbon plays based on Jurassic source rocks in rifted, necked zone and on Jurassic oceanic crust along with Cretaceous sources underlying clastic reservoirs in late Cretaceous submarine fans.

Nima Khorshidian

Cloud Formation and Precipitation over Texas: Improving Model Simulations using Observation Nudging and Detailed Microphysics

This study presents an in-depth evaluation of the Weather Research and Forecasting model coupled with Chemistry (WRF-Chem) over Texas by employing various microphysics schemes and observation nudging techniques. The aim is to assess the model's performance in simulating meteorological parameters such as temperature, wind speed, and radar reflectivity. The project began with the implementation of the WRF-Chem model over CONUS using 12 km horizontal grid spacing. A nested domain was then set up over Texas with a finer resolution of 4 km to facilitate detailed analysis. The Morrison two-moment bulk microphysics scheme was employed for the larger domain, which also provided initial and boundary conditions for the nested domain. Four distinct scenarios were designed to run the model over Texas. Two scenarios utilized the Morrison bulk microphysics scheme, while the other two employed the spectral bin microphysics scheme. Each microphysics scheme was tested with and without observation nudging, resulting in four unique configurations. To perform observation nudging, National Centers for Environmental Prediction (NCEP) surface and upper air observation data were incorporated. Model outputs were compared with observational data from the Air Quality System (AQS) network and the Next-Generation Weather Radar (NEXRAD) in Texas. The AQS data were utilized to validate temperature, while NEXRAD radar reflectivity data were employed to evaluate the model's performance in capturing radar reflectivity patterns. This comprehensive evaluation of WRF-Chem over Texas using multiple scenarios and microphysics schemes sheds light on the model's ability to accurately simulate meteorological parameters. The outcomes of this study provide valuable insights for the scientific community and model developers, ultimately contributing to the improvement of weather and air quality forecasting.

Sai Udaya Meghana Yella

A study on Helium

The objective of this project is to study the properties of Helium gas and the availability in United States. It is the first member of the noble gas group in the periodic table and is a transparent, odorless, tasteless, non-toxic, inert, monatomic gas. Many advancements have been made to use Helium gas in different sectors, but the research is going on to find if it can be used as a fuel or not. The data of Helium hotspots have been gathered from USGS website and mapped with the help of Arc GIS software. A sandstone sample is saturated with Helium gas and the velocity of it is calculated. The behavioral characteristics of it are to be known first. This also helps to understand the gas properties inside a sandstone rock. The sample is a Berea , it is placed in ahigh pressure chamber with axial , confining pressure and the setup has a mineral oil enclosed in a tank to recreate reservoir. The pore pressure is increased gradually to let the rock absorb more of the gas. The Vs and Vp of the rock are measured at the benchtop and after the experiment. Also, the velocity of Helium with respective to different temperatures and densities are predicted with FLAG software and compared with the lab readings.

Sharmila Appini

Intra-slab anisotropy beneath Japan through Shear Wave Splitting

Strong intra-slab seismic anisotropic fabric of laminated type (~25% shear anisotropy) within the vicinity of deep subduction earthquakes (focal depth > 60 km) was proposed to explain the cause of the large non-double-couple radiation patterns. If it is true, a predicted consequence is that the dipping anisotropic slab should produce shear wave splitting (SWS). Due to the dipping geometry, the measured splitting parameters (delay time and polarization directions) should depend on incident angles of the S-wave ray paths with respect to the slab. We evaluate this prediction by analyzing teleseismic waveforms of around ~600 global earthquakes recorded by a dense network coverage (>800 Hi-net stations) in Japan. After acquiring >8,000 high-quality SWS measurements for various S phases (S, ScS and SKS), we explore SWS patterns using the event backazimuth, focal depth, and forward seismic modeling. Our measured results indicate that the delay time between the fast and slow shear waves vary significantly up to ~3 s but also with numerous null measurements (~950 observations). In addition, the measured fast S polarization direction has a complex but systematic relation with respect to the source location and depth, likely due to source-side anisotropy weakening with event depth. We also notice a spatial variation of the measured SWS patterns across Japan for the same earthquake, showing the influence of Pacific and Philippine Sea slabs on SWS which cannot be attributed to source-side anisotropy. Finally, we perform seismic forward modeling using the propagator matrix method to explain these measurements. We find that a 20km thick anisotropic layer in the slab can cause similar delay times and a systematic rotation of the fast S polarization axis. These outcomes show that in teleseismic SWS analyses, we need to consider the dipping anisotropic slab, not just the sub/supra-slab anisotropy and earthquake source side anisotropy. Our approaches and analyses provide new tools for understanding slab anisotropic structure, important for deep earthquake generation and recycling of volatiles back into the Earth mantle.

Undergraduate - Oral Presentations

Aliasghar Shariff

Auroral Spectroscopy

The Aurora Borealis, or the Northern Lights, is a magnificent display of colorful lights found by the North Pole, created by electromagnetically charged particles emitted from the sun colliding with gasses in the Earth's atmosphere. The brilliant colors correspond to the variety of atmospheric molecules, and the aurora varies in brightness or intensity, as related to the energy of the ionizing particles. The goal of this experiment is to identify specific, known spectral lines emitted by the aurora borealis, using student-designed and made emission spectroscopes, which will take images of the aurora partially in the ultraviolet-visible (350-700 nm) and infrared (700- 1100 nm) ranges. Via auroral spectroscopy, the presence and properties of atmospheric molecules such as molecular oxygen, which forms the well-known "auroral green line" at 557 nm, atomic oxygen which has a strong line at 771 nm, and atomic nitrogen which has a few strong lines in the 424-428 nm range, as well as many others, in the proper conditions. Spectroscopy is a diverse science, and emission spectroscopy is a method in which the wavelength of the emitted light is measured. Every molecule, and the energy level of that molecule, will show specific lines when viewed with a spectroscope, known as its spectra. Hence, emission spectroscopy has many applications in the astronomical and atmospheric sciences. With the increased sensitivity of instruments and ease of construction, this method has the potential not only to identify large amounts of atmospheric gasses but to detect trace amounts of pollutants and other contaminants as well. The Undergraduate Student Instrumentation Project (USIP) is a university-run research program led by Dr. Edgar Bering that creates balloon-borne and ground-based instruments to study the upper atmosphere and the aurora borealis. There are five instrument teams, one of which is the Auroral Spectroscopy team. The design of this experiment consists of a Newtonian telescope to which a spectrophotometer is attached. The spectrometer will split the light into the observed molecules' spectra using a series of lenses for focusing the light into a real image, a slit, and a transmission diffraction grating lens. The spectroscope will be further attached to a full-spectrum camera that will capture an image to be processed. The images captured of auroral sessions will be analyzed to obtain wavelength and intensity data, which will inform us of the energies of the observed molecules. This experiment grants the opportunity to study our atmosphere in a unique and accessible way, as well as resulting in data that will contribute to the spectral study of the Aurora Borealis

Borna Koohbor

The Impacts of Temperature and Humidity on the Light Scattering Properties of Sulfur-derived and Calcite Aerosols

In this experiment, we aim to discover the optical properties of aerosols using a Nephelometer, an instrument designed to measure the light scattering properties of a gaseous or liquid medium. Our nephelometer works alongside a custom-designed climate control system that allows for conditions down to -80 degrees Celsius and a full range of relative humidity values. The control system utilizes a stainless steel loop connected to control checkpoints, such as a humidity checkpoint. The temperature control outside this loop uses a dry ice bath and liquid pump. Our focus is on the aerosols of sulfuric acid and calcite. We wish to understand how the scattering properties of these aerosols vary with temperature and humidity. Scattering properties depend on the aerosols' physical characteristics, such as size, shape, and molecular structure. Understanding the full extent of spreading properties can inform geoengineering decisions, where aerosols are frequently cited as a temporary solution for rising temperatures.

Celine Saidy

Gaseous Compounds: Measuring the Composition of Trace Gasses in Earth's Atmosphere

The composition of the Earth's atmosphere is integral to the state of our planet. The general composition of the atmosphere has been recorded and verified multiple times, and it is well known that the most abundant gasses in the atmosphere are elemental Nitrogen, Oxygen, and Argon, followed by Carbon Dioxide. However, the atmosphere also contains trace amounts of various other compounds, as well. The purpose of this experiment is to measure the presence of trace gasses in the atmosphere. Over the past few decades, human activity has had a worrisome effect on Earth's atmospheric composition. As a result, there is an increasing need to study the changes in the atmosphere. In a previous iteration of the project, collecting data on the presence of trace gasses was attempted; however, an error in one sensor meant that it was left incomplete. In this iteration of the experiment, a payload consisting of various sensors will be launched into the atmosphere via a balloon-borne payload. These sensors will be used to measure the abundance of NO, NO2, SO2, SH2, CO, and O3. A vacuum pump will be used to bring air into the payload, upon which the sensors will analyze its composition. Through this experiment, we hope to obtain a proper reading on the presence of various important trace gasses, so that we can analyze it in comparison to known trends and determine where we currently stand regarding the health of our planet's atmosphere.

Faith Walton

Structural restoration and driving forces for the Oligocene-Recent opening of the Gulf of California

The Gulf of California is the body of water between the Baja Peninsula and mainland Mexico. This region is an oblique rift zone along the boundary between the Pacific and North American plates. The active passive margin opened during a period of Late Miocene (12.5 Ma) to Recent oblique separation movement, accommodated by right-stepping en-echelon, strike-slip, and oblique faults, that offset strain along narrow pull-apart basins between the North American and Pacific plates (Bennet et. al. 2014). The proto-gulf era, beginning around 12.5 Ma and ending around 6 Ma, was onset by the southward migration of the Rivera Triple Junction, causing the tectonic setting to evolve to a dextral transition motion and marked a transition of plate motion to the western edge of the province (Atwater et. al. 1998). Marine incursion, which formed the continuous gulf that we are familiar with today, occurred around 6.5-6.3 Ma (Oskin et. al 2003). This study uses reconstructions of seismic refraction sections done using the Area Error Prop software and methods from Nguyen et. al and slab mapping done using tomography data from Simmons et. al 2012 and Persaud et. al 2016 and GoCad software. Comparing the extension rates throughout the gulf by reconstructing sections of seismic refraction lines across key basin systems to a mapped remnant slab beneath the western edge of the peninsula gives insight on how subducted slab remnants affect the extension occurring in the basins.

Jason Ruszkowski

Sampling Microplastics and Extremophile on Balloon Borne Payloads

The Microplastics and Extremophiles team under the University of Houston's Undergraduate Student Instrument Project intends to launch an instrument to collect microplastics and extremophiles within the stratosphere between 15 km and 30 km above Utopia, Texas. The team is also planning on the use of several ground collecting instruments both in Utopia, and Houston, Texas, that will measure microplastics by precipitation and deposition. The balloon platform was selected for its low speed, high altitude, and long flight time. This flight would ascend to about 30 km, and provide at least half an hour of measurement time within the desired altitude range. The instrument itself would consist of a lightweight, mylar bellows system, driven by pulleys. This design meets the high flow rate requirements to achieve the largest feasible sample, while maintaining the lightest weight. Raman spectroscopy will be utilized for analyzing microplastics while samples of extremophiles will be analyzed via PCR and 16S rRNA sequencing. The team has already collected sample data from Fairbanks, Alaska, and is currently in the process of building a Pi-Raman spectroscope for analysis.

Graduate Posters

Divine Kalu

Uncertainty Quantification of 3D Electromagnetic Inversion Using Invertible Neural Network

Solving inverse problems is always complicated as a result of its non-uniqueness and ambiguity. This means that there are many possible models that can give rise to the same observed data. As such, quantifying the uncertainty of inverse solutions becomes important as it allows us to understand which inverted features are more reliable and which are less. One common method for estimating the uncertainty is the Bayesian inference which often involves random sampling in a high dimensional space. However, the sampling process can be computationally expensive for 3D inverse problems involving hundreds of thousands to tens of millions of model parameters. We propose a different approach - the Invertible Neural Network – to evaluate the model uncertainty. The INN is unique as it provides a bijective mapping between the inputs and outputs and this creates a somewhat natural way of solving inverse problems. The network doesn't require an explicit backward training since the network architecture is created in such a way that, after training the network on a well understood forward process, we can easily obtain the solutions of the inverse problem by running the trained network in the reverse direction. To help account for the information loss during the forward process, a latent variable (z) is added to the output (d) and this creates a unique pair [d , z] which enforces the bijectivity (one-to-one mapping) of the network. As a proof of concept, we have applied this method to a 1D surface wave dispersion problem. Our preliminary results show reasonable results and good potential in generating many samples of the posterior distribution in a computationally efficient way. Our next step is to extend the method to 3D inverse problems of magnetotellurics data with applications to critical minerals and geothermal exploration.

Geoffrey Roberts

2021 September Model Intercomparison between WRF-gc, WRF-chem and CAMx to observed data

This is a model intercomparison with the 2021 TRACER-AQ 1 campaign comparing 3 different models for the month of September. TRACER-AQ 1 (Tracking Aerosol Convection interaction ExpeRiment) is a campaign run by the Atmospheric Radiation Measurement (ARM) user facility under the U.S. Department of Energy Office of Science. The purpose of this campaign is to learn more about the cloud and aerosol interactions in deep convection over the Houston area. This is done with the use of the ARM Mobile Facility (AMF1), the second-generation C-Band ARM precipitation radar (CSAPR2), and a small satellite site with radiosonde and aerosol measurements.

I will be doing a model intercomparison between observed data pulled from the TCEQ (Texas Commission on Environmental Quality) website and data from 3 model (WRF-gc, WRF-chem, and CAMx) for ozone. Each of the models are run with the same chemistry parameters at a 1km spatiotemporal resolution. WRF-gc and CAMx use HRRR for their meteorology conditions while WRF-chem uses GFS. All concentration units have been converted to ppbv (parts per billion volume) and all data has been converted to local time. Observation data from 25 sites was used for the comparison with all data being at ground level. A vertical profile comparison was also done to analyze boundary conditions. For vertical profile comparison, observation data was omitted and hPa was used as the height units for each model. Data was averaged daily and then over the whole month.

Initial analysis of the data showed all models higher than the observed data, with WRF-gc showing the highest bias. A clear correlation on whether high ozone days or clean days where worse could not be determined. High ozone was also reported over the Gulf of Mexico and in certain areas at night. Initial vertical profile comparison showed slight deviation between the models above the boundary layer, but further analysis is needed.

Future work includes running a statistical analysis on the observed vs model ground level data, gathering ozonesonde data and running a comparison with the vertical profile data, looking into daytime vs nighttime ozone correlations, and looking into high and clean ozone days.

Irfan Karim

Impact of Covid-19 lockdown regulations on PM2.5 and trace gases (NO2, SO2, CH4, HCHO, C2H2O2 and O3) over Lahore, Pakistan

The COVID-19 pandemic altered the human mobility and economic activities immensely, as authorities enforced unprecedented lock down regulations. In order to reduce the spread of COVID-19, a complete lockdown was observed between 24 March – 31 May 2020 in Pakistan. This paper aims at investigating the PM2.5, AOD and column amounts of six trace gases (NO2, SO2, CH4, HCHO, C2H2O2 and O3) by comparing periods of reduced emissions during lockdown periods with reference periods without emission reductions over Lahore, Pakistan. HYSPLIT cluster trajectory analyses were performed, which confirmed similar meteorological flow conditions during lockdown and reference periods. This provides confidence that any change in air quality conditions would be due to changes in human activities and associated emissions. The results show about 38% reduction in ambient surface PM2.5 levels during the lockdown period. This change also positively correlated with MODISDB and AERONETAOD data with a decrease of AOD by 42% and 35%, respectively. Reductions for tropospheric columns of NO2 and SO2 were about 20% and 50%, respectively during a semi lockdown period, while no reduction in the CH4, C2H2O2, HCHO and O3 levels occurred. During the lockdown period NO2, O3 and CH4 were about 50%, 45% and 25% lower, respectively, but no reduction in SO2, C2H2O2 and HCHO levels were noticed compared to the reference lockdown period for Lahore. HYSPLIT cluster trajectory analysis revealed the greatest impact on Lahore air quality through local emissions and regional transport from the east (agricultural burning and industry).

Jincheol Park

The Sensitivities of Ozone and PM2.5 Concentrations to the Satellite-Derived Leaf Area Index over East Asia and its Neighboring Seas in the WRF-CMAQ Modeling System

Vegetation plays an important role as both a sink of air pollutants via dry deposition and a source of biogenic VOC (BVOC) emissions which often provide the precursors of air pollutants. To identify the vegetation-driven offset between the deposition and formation of air pollutants, this study examines the responses of ozone and PM2.5 concentrations to changes in the leaf area index (LAI) over East Asia and its neighboring seas, using up-to-date satellite-derived LAI and green vegetation fraction (GVF) products. Two LAI scenarios that examine (1) table-prescribed LAI and GVF from 1992-1993 AVHRR and 2001 MODIS products and (2) reprocessed 2019 MODIS LAI and 2019 VIIRS GVF products were used in WRF-CMAQ modeling to simulate ozone and PM2.5 concentrations for June 2019. The use of up-to-date LAI and GVF products resulted in monthly mean LAI differences ranging from -56.20% to 96.81% over the study domain. The increase in LAI resulted in the differences in hourly mean ozone and PM2.5 concentrations over inland areas ranging from 0.27 ppbV to -7.17 ppbV and 0.89 μg/m3 to -2.65 μg/m3, and the differences of those over the adjacent sea surface ranging from 0.69 ppbV to -2.86 ppbV and 3.41 μg/m3 to -7.47 μg/m3. The decreases in inland ozone and PM2.5 concentrations were mainly the results of dry deposition accelerated by increases in LAI, which outweighed the ozone and PM2.5 formations via BVOC-driven chemistry. Some inland regions showed further decreases in PM2.5 concentrations due to reduced reactions of PM2.5 precursors with hydroxyl radicals depleted by BVOCs. The reductions in sea surface ozone and PM2.5 concentrations were accompanied by the reductions in those in upwind inland regions, which led to less ozone and PM2.5 inflows. The results suggest the importance of the selective use of vegetation parameters for air quality modeling.

Kenneth Shipper

Basin modeling based on crustal structure reveals productive hydrocarbon trends along the Guyana-Suriname rifted-passive margin

Differences in crustal type (more radiogenic and warmer sialic continental crust vs. less radiogenic and cooler, mafic oceanic crust), crustal thickness (full-thickness, rifted, and oceanic) and overburden thickness all play an important role in the variations in heat flow and maturation of hydrocarbons along rifted-passive margins. Using a crustal model from 3D gravity inversion, I calculate radiogenic heat production (RHP) from the Guyana-Suriname rifted-passive margin to constrain a full-lithospheric, thermal-transient models that reveal productive hydrocarbon trends along the entire margin. The crustal structure non-volcanic segment of the northwest Guyana basin provided by the crustal model indicates a 170-km-wide transition from: 1) a pre-rift thickness of 40-50 km in the Guiana cratonic shield to; 2) a rifted continental crust thickness in the necked zone of 10-30 km; and to a late Jurassic oceanic crust of 6-8 km in the deepwater Guyana basin. The crustal model from 3D gravity inversion converges to 1 mGal with a 1 km error to its nearest refraction controls. Towards the southeast, the non-volcanic Guyana margin transitions to the Demerara volcanic margin in Suriname that is characterized by thick, 25-km-thick seaward dipping reflectors and formed as a late Jurassic (197-173 Ma) plume head and hotspot track coeval with the non-volcanic rifted margin of northwest Guyana. I use five wells across both areas to the values of radiogenic heat production (RHP) values and geothermal gradients at 5.25 km below mudline for these crustal provinces: 1) rifted, non-volcanic necked zone in northwest Guyana (RHP = 46-12 mW/m^2 and geothermal gradient = 48 °C/km); 2) rifted, volcanic necked zone on the Demerara Plateau of Suriname (16 mW/m^{2}and 14-19 °C/km); and 3) oceanic crust of the deep Guyana basin (0 mW/m^{2}and 5 °C/km). I then use these inputs to constrain maturity maps for the known Cenomanian-Turonian source rock for this margin. The predicted maturity map is validated by comparison to the distribution of known oil and gas discoveries along with the areas of known dry holes.

Larkin Spires

Empirical Determination of the Effective Solid Modulus in Organic-Rich Shales

Calculating the change in the saturated bulk modulus of a saturated rock as fluid properties change requires a priori selection of an effective bulk modulus of the solid constituents. When mineral moduli are similar, theoretical bounds on the solid modulus are tight. However, when solid properties vary greatly, as in organic-rich shales, bounds on the effective solid modulus result in uncertainty in the predicted change in the saturated bulk modulus of the rock. We use a semi-empirical rock physics model utilizing the Brown-Korringa equation for polymineral assemblages and introduce three parameters to estimate the pore space compressibility, the dry frame compressibility, and the fractional position of the effective solid modulus relative to the Reuss and Voigt bounds. We optimize for these three parameters in seven organic shale formations and find that the Reuss bound for the effective solid material modulus best fits the data when organic content is high. Furthermore, we use this model to fluid substitute to 100% brine saturation and find Gassmann's equation using the Hill average predicts similar saturated moduli to the semi-empirical Brown-Korringa rock physics model when volume fraction of solid organic matter is less than 5%. However, at higher organic contents, we find that the error using the Gassmann-Hill approach increases, and the semi-empirical Brown-Korringa model better fits the data.

Lisabeth Arellano

Can we use precipitation totalizers for triple oxygen isotope studies in hot, dry environments?

The emerging $\Delta'^{17}O$ hydrological tracer holds the potential to provide new information regarding paleoclimate from proxy materials such as ice cores and speleothems, evapotranspiration from leaf and stem water, and general evaporative regimes from liquid waters beyond the traditional stable isotope parameters δD, $\delta^{18}O$, and d-excess. Understanding the mechanisms that drive $\Delta'^{17}O$ variations in modern waters is the first step to expounding the utility of these measurements. However, none of the "totalizers" designed to collect a single precipitation sample pooled over a calendar month and prevent or minimize evaporation and associated isotopic fractionation of the sample during that time have been tested for their ability to preserve $\Delta'^{17}O$. Here we present a 30-day laboratory experiment using four totalizers: 1) the classic oil-based collector, 2) the commercially available tube dip-in/pressure equilibration collector, 3) a new collector created as an addition to the ATMOS41 weather station by the OSU OPEnS lab, and 4) a reference collector (the control). The collectors were filled to 12% of their volume with deionized water from Houston and placed in a modified laboratory oven with a diurnal temperature change of 24 to 40°C and an average relative humidity of 10%. Mass losses from each totalizer were determined daily and samples were taken every three days for isotopic analysis. At the end of the experiment, the reference collector showed the biggest mass loss (5.8 g or 2.4% of its original mass), followed by the tube dip-in collector (5.0 g or 1.4% of its original mass), the oil collector (1.5 g or 0.6% of its original mass), and finally, the OPEnS collector (0.7 g or 0.2% of its original mass). The reference and tube dip-in collectors experienced $\Delta'^{17}O$ shifts of -266 per meg and -41 per meg, respectively, while the oil and OPEnS collectors stayed within $\Delta'^{17}O$ analytical precision (shifts less than ±15 per meg). For nine days, the OPEnS collector was the only collector to stay within δ18O analytical precision (a shift less than 0.025‰), suggesting that a weekly sampling strategy using the OPEnS collector is ideal for both triple oxygen isotope and traditional isotope studies in arid settings. However, the triple oxygen isotope changes associated with oil and tube dip-in collectors may still be acceptable for studies in more humid environments employing a monthly sampling strategy given the extreme conditions of our experiment.

Madison Rafter

Paleosol Core-lations in Baringo Basin, Kenya: Impacts on Early Hominin Environments in the Eastern African Rift

The BTB13 sediment core drilled in Baringo Basin– located in the Eastern African Rift– consists of alternating lacustrine and fluvial strata with numerous ancient soils (paleosols) dating from 3.29 to 2.56 Ma. Early hominins relied on paleolakes like Baringo for food, water, and vegetation. Paleosols provide important context for paleoenvironmental and paleoclimatic conditions through physical paleosol characteristics (i.e., color, carbonate presence, and micromorphological features). Although the BTB13 core has been analyzed previously for the initial core description, leaf wax biomarkers, lacustrine diatoms, tephra chronostratigraphy, and lacustrine phytolith assemblages, the paleosols were not the target of these studies despite their presence in 57% of the core. Here, we update the stratigraphy of the BTB13 core recording paleosol thickness, depth, and characteristics. We then correlated the core record with previous outcrop work in Baringo Basin on outcrops known as B-B', T-T', and NET using tephra dated in previous chronostratigraphic works and by correlating five laterally-persistent diatomite layers present in both the outcrop and the BTB13 core. Future sampling and paleoclimate reconstructions for the BTB13 core will benefit greatly from the correlation of these units. Samples from both outcrop and core will be analyzed for bulk geochemistry and bulk organic matter. We will use stable (C and O) and clumped isotopes (Δ47) from pedogenic carbonates in the paleosols to track changing seasonality and aridity and to determine paleotemperatures during carbonate formation. I will also analyze the bulk and clay mineralogy of the paleosols using X-ray Diffraction to characterize paleoaridity and soil fertility via saline mineral abundance. Physical characteristics, mineralogy, and chemistry of paleosols along the lake margin or during low-lake periods will provide valuable information about the suitability of the environment for early hominins because soil salinity and mineralogy affects type and quality of vegetation. Salinity should increase when evaporation exceeds precipitation, thereby decreasing paleosol fertility. Future work from these Baringo Basin core and outcrop correlations will show laterally shifting marginal lacustrine environments via the marginal paleosols and lacustrine units to provide a clearer picture of how environmental change impacted the evolution of early hominins in the Eastern African Rift.

Mahsa Payami

A 1D CNN-based Digital Twin for CMAQ: Predicting NO2 Concentration over the most populated cores in Texas.

In this study, we designed a digital twin for the Community Multiscale Air Quality (CMAQ) model using a 1D Convolutional Neural Network (CNN) deep learning algorithm to predict hourly surface NO2 concentration for the most populated cores in Texas. We achieved an Index of Agreement (IOA) of 0.95 and accuracy of 0.91, demonstrating the effectiveness of our approach in accurately predicting hourly surface NO2 concentration. Furthermore, we used Shapley Additive Explanations (SHAP) analysis to gain insights into the model's inner workings. We also compared the computational time between CMAQ and our digital twin, and found that our digital twin was 390X faster in predicting NO2 concentration. The results of our study could serve as a valuable tool for policy-makers and stakeholders in mitigating air pollution in Texas, as the digital twin could be used to provide real-time and high-resolution NO2 concentration estimates. Additionally, the faster computational time of the digital twin could enable more efficient decision-making and improve public health outcomes.

Mayra Lopez Carrasquilla

Ultrasonic measurements of elastic anisotropy of granitic rocks for enhanced geothermal reservoirs

Intrinsic elastic anisotropy properties of foliated and non-foliated granites are important for enhanced geothermal systems to determine subsurface stress states. We perform lab experiments to measure P- and S-wave velocities to determine the seismic anisotropy. The ultrasonic sounding assembly (transducer-sample-receivers) measures velocity and amplitude on the cylindrical sample in three independent directions. Observed velocity changes and attenuation with increasing confining pressures in a range of 5 to 50 MPa at room temperature. The effects of increasing pressure on the directional dependence of velocity and the Q-factor were investigated in five directions. The measured anisotropy values of the foliated granite sample for P-wave velocity are more than 22% and for S-wave is more than 13%.

Moloud Rahimzadeh

Assessing large-scale mantle compositional heterogeneity from machine learning analysis of 28 global P- and S-wave tomography models

Differences between P- and S-wave models have been frequently used as evidence for the presence of large-scale compositional heterogeneity in the Earth's mantle. Our two-step Machine Learning (ML) analysis of 28 P- and S-wave global tomographic models reveals that, on a global scale, such differences are for the most part not intrinsic and could be reduced by changing the models in their respective null spaces. In other words, P- and S-wave images of mantle structure are not necessarily distinct from each other. Thus, a purely thermal explanation for seismic structure is sufficient at present; significant mantle compositional heterogeneities do not need to be invoked. We analyze 28 widely-used tomographic models based on various theoretical approximations ranging from ray theory (e.g., UU-P07, MIT-P08), Born scattering (e.g., DETOX) and full-waveform techniques (e.g., CSEM, GLAD). We apply Varimax Principal Component Analysis to reduce tomography model dimensionality by 83% while preserving relevant information (94% of the original variance), followed by hierarchical clustering analysis (HC) using Ward's method to categorize all models into a hierarchy of groups based on similarities. We found two main tomography model clusters: Cluster 1, which we called 'Pure P-wave', is composed of six P-wave models that only use longitudinal body wave phases (e.g., P, PP, Pdiff); Cluster 2, which we called 'Mixed', includes both P- and S-wave models. P-wave models in the 'Mixed' cluster use inversion methods that include inputs from other geophysical and geological data sources, which cause them to be more similar to S-wave models than to pure P-wave models without a significant loss of fitness to P-wave data. Therefore, most differences between tomographic models can be removed by moving both models within their respective null spaces. Inclusion of new data classes and seismic phases in more recent tomographic models significantly change the imaged seismic structure.

Nina Zama

Thermal decomposition, coseismic and interseismic microstructures of carbonate fault rocks: Insights from Hebgen Lake earthquake rupture, Montana

Seismic slip in carbonate rocks can cause the decomposition of carbonate minerals such as dolomite, calcite, and siderite due to frictional heating at temperatures of around 600ºC. The main decarbonation reactions are:
CaMg(CO3)2 <->CaCO3 + MgO + CO2 [Dolomite <-> Calcite + Periclase + Carbon Dioxide], CaCO3 <-> CaO + CO2 [Calcite <-> Lime + Carbon Dioxide], 3 FeCO3 <-> Fe3O4 + 3 CO2 [Siderite <-> Magnetite + Carbon Dioxide]
This results in the production of significant amounts of CO2, either in gaseous or supercritical fluid form, which rapidly reduces friction along the slip plane. Decarbonation, therefore, plays a crucial role in controlling the mechanical behavior and slip of seismogenic faults in carbonates. I investigate the thermomechanical processes associated with decarbonation by using microstructural analysis combined with rock magnetism. The Hebgen Lake Fault, which experienced a Mw 7.2 earthquake in 1959, with a vertical displacement of approximately 7.7 m along a steep normal fault across the Cambrian Meagher Limestone in Montana, is used as an example of extreme deformation events in carbonates. New field observations were made on a uniquely preserved bedrock fault scarp and discovers the presence of patchy layers of barely deformed botryoidal goethite near the fault plane, with hematite slickensides forming extensive fault mirror surfaces. The author suggests that the formation of botryoidal concretions likely occurred during interseismic/aseismic periods due to precipitation from an iron-rich fluid. The abrupt transition from goethite to hematite indicates that the latter formed through frictional-heating dehydration of goethite. This interpretation is further supported by the measurement of the anisotropy of magnetic susceptibility (AMS). The measured AMS slip direction is consistent with the slickenside orientation and thus represents the direction of seismic slip. The transformation of goethite to hematite suggests that frictional heating occurred on the fault mirror at a local temperature of at least 200ºC, which is probably just below the onset of decarbonation.

Ronin Costello

A high resolution modeling study of meteorologically and chemically driven ozone exceedance events in the Houston Galveston Brazoria region

This study investigates chemistry model performance of surface ozone forecasting in the Houston Galveston Brazoria (HGB) region during September 2021. The spatial variation in ground-level ozone is often related to changes in land use. The HGB region is an urbanized region that experiences urban warming, which can enhance heat-stress and ozone levels through photochemical reactions. Multiple in-situ observational measurements, the Weather Research and Forecasting (WRF) GEOS-Chem (GC) Model version 3.9, the WRF-Chem Model version 4.3, and the Comprehensive Air Quality Model with Extensions (CAMx) Version 7.10 are used. The simulations were performed over 3 nested domains with the finest being at 1.33 km. 3 ozone exceedance periods were identified in September 2021: September 6-11, September 17-19, and September 23-26. The rest of the days in September 2021 are collectively known as the clean ozone period. Overall, each model reproduced the spatiotemporal variations on ozone over the HBG, but distinct biases are found in a time of day analysis. Observation site-averaged ozone model bias is greater in the mornings of both high and clean ozone days than the afternoon (~10 ppbv bias to ~4 ppbv) when averaged across each of the models. The average ozone bias for each model is lower during high ozone periods than clean ozone periods, consistent with previous chemistry model studies that show underestimation of ozone during high ozone periods and overestimation of ozone during clean ozone periods. CAMx displayed the best overall ozone forecasting during the month. Correlation analysis of the morning ozone biases (700 CDT 1100 CDT) and afternoon ozone biases (1200 CDT - 1700 CDT) was on an observation site to observation site basis to determine whether significant spatiotemporal shifts in ozone forecasts during the day. Morning and afternoon biases were correlated most strongly with CAMx (~R=0.62). Consistency is displayed in all 3 models because correlations were weak and positive for each of them. Future work will be done to determine more of the chemical causes behind the temporal biases and how the bias shift in a diurnal cycle

Sara Rojas

Investigation of Fluid Pressure Distribution in Poroelastic Media with Variable Porosities

Subsurface rocks have spatially variable porosities. To investigate the fluid pressure distribution in heterogeneous poroelastic material, we model Biot's equations via a staggered grid velocity-stress finite-difference scheme. We have observed in our modeling that waves slow down when traveling from low-porosity regions to high-porosity regions. This offers a possibility of energy focusing which can enhance the pore fluid pressure. New results will be shown on the amount of pressure amplification and whether such an effect can cause liquefaction and triggered earthquakes.

Xinyue Wang

Variations of Carbonyl Sulfide During the Dry/Wet Seasons Over the Amazon

Mid-tropospheric Carbonyl sulfide (OCS) retrievals from the Tropospheric Emission Spectrometer (TES) are utilized to study OCS distributions during the dry/wet seasons over the Amazon rainforest. TES OCS retrievals reveal positive OCS anomalies (~16 ppt) over the central and southern parts of the Amazon during August–October (dry season) compared to January–March (wet season). There is less OCS taken up by vegetation and soil and more OCS released from biomass burning during the dry season, which causes an increase in OCS concentrations. Strong sinking air during the dry season also helps to trap OCS and this contributes to positive OCS anomalies. MOZART-4 model captures positive OCS anomalies over the central and southern regions of the Amazon and negative OCS anomalies over the northern part of the Amazon, which are similar to those from TES mid-tropospheric OCS retrievals. Our studies can help us better understand OCS variations and photosynthetic activities.

Undergraduate Posters

Emily Stivison

Grain Size Analysis of Sandstones from the San Juan Basin, New Mexico, USA

Ongoing research in the San Juan Basin, New Mexico, USA, is being conducted to study the effects of early Eocene climate change in mid-low latitudes in North America to help expand our understanding of how global warming drives changes in monsoon intensity, extreme rainfall events, and landscape response in North America. The San Jose Formation, found in the San Juan Basin, is the most extensively preserved and exposed Eocene unit in New Mexico. Here we present data from two members of this formation, the Cuba Mesa and Regina Members, which in some places unconformably overlies the Paleocene Nacimiento Formation. Sandstone samples used to conduct this research are from the Arroyo Chijuilla and Continental Divide West sites. Grain size and grain shape was analyzed using a Cilas 1190 Laser Particle Size Analyzer at the University of Houston. Sixteen samples were used to help determine provenance, distance of transport, and flow regime based on their stratigraphic position. Preliminary data shows an increase in precipitation variability and likely an increase in river discharge. Future work will tell us more about changes through time between grain shape and the formation, transportation, and deposition processes of the sandstones.

Johanna Villagomez

Using GPS to Monitor Subsidence and Faults in the Greater Houston Area

The Greater Houston area has been experiencing ground deformation for nearly 100 years due to subsidence and faults. The results of this subsiding and faulting has caused damages to commercial, residential, industrial buildings and public infrastructure. These damages are generally overlooked until an extensive area is affected and significant collateral risks have been induced. Since the 1990s GPS technology has become the primary tool for monitoring subsidence in the Greater Houston area. This technology was implemented by the collaboration of National Geodetic Survey (NGS) and Harris-Galveston Subsidence (HGSD.) Shallow aquifers which consist of interbedded clays, silts, sand and gravels are experiencing excessive amounts of groundwater withdrawals which leads to the main cause of land subsidence in Greater Houston area. The major aquifers belong to the gulf coast aquifer system, from the land surface downward, including Chicot aquifer system, the Evangeline aquifer, the Burkeville conning unit, the Jasper aquifer, and the Catahoula sandstone. Precise monitoring of ground deformation over a long period of time is essential to managing ongoing geological hazard as it relevant to plans for the future development of urban areas. These long term observations can also contribute ground deformation truth and calibration data that can be used for multiple remote sensing tequnies and subsidence modeling. Beginning in 1975 the Texas Legislature created HGSD, which is divided into Area1, Area 2 and Area 3. Fort Bend Subsidence District (FBSD) in 1989 which is divided into Area A and Area B. Lone Star Groundwater Conservation District (LSGCD) in 2001, and Brazoria County Groundwater Conservation District (BCGCD) in 2005. In cooperation which one another University of Houston (UH), FBSD,LSGCD, BCGCD, and other local institutes, HGSD has accumulated about 250 permanent GPS stations within the Greater Houston Region into its regular subsidence monitoring. The combination of all the publicly available stations is called HoustonNet. The Geodetic Laboratory at UH has been responsible for the HoustonNet data Process and analysis since 2016.

Joseph McNease

Investigation of Fluid Pressure Distribution in Poroelastic Media with Variable Porosities

Subsurface rocks have spatially variable porosities. To investigate the fluid pressure distribution in heterogeneous poroelastic material, we model Biot's equations via a staggered grid velocity-stress finite-difference scheme. We have observed in our modeling that waves slow down when traveling from low-porosity regions to high-porosity regions. This offers a possibility of energy focusing which can enhance the pore fluid pressure. New results will be shown on the amount of pressure amplification and whether such an effect can cause liquefaction and triggered earthquakes.

Leo Collier

Barringer Crater; Recreating Anomalous Impact Morphology through Sandbox Modelling

Barringer (Meteor) crater, Arizona is one of the most well studied impact craters on the Earth's surface. The cause of its unusual square shape has been hotly debated for many decades and not yet settled. This research investigates a range of geologically related aspects that may help solve the mystery of its anomalous shape. We consider various geologic factors that could influence the course of the impact crater's ultimate shape: 1) an anisotropic (patterned) host rock, 2) aligned fractures and faults in the rock, 3) anticlinal structure, 4) an asymmetric horizontal stress regime. In addition, a non-spherical impactor might play a role as well. We have undertaken a variety of scaled physical modeling tests (small firecracker explosions in sandy materials) with materials and structures to test the above possible sources of asymmetry. We find that structures and stresses have an effect on the final crater shape. In particular, an anticlinal host material creates an asymmetric crater after impact as does an unbalanced horizontal confinement. We are preparing "tiled" models with square and rectangular tiles to test their effect on resultant craters. In addition, we are working with NASA's hypervelocity projectile system to further understand the effect of bolides impacting asymmetric materials.

Noelle Cheshire

Mitigating the Anthropogenic Effects of Factory Farming on Terrestrial Resources, Atmospheric Pollution, and Human Health.

Factory farming is one of the most prominent infrastructures associated with human-induced climate change as a direct consequence of increased greenhouse gas (GHG) emissions, soil degradation, water pollution, destruction of ecological dynamics and loss of biodiversity. Despite the biosphere stressors linked to industrial agriculture it is still expanding due to rapid population growth and adaptation of western dietary patterns. Meat production specifically affects the sustainability of these agroecosystems at a disproportionate rate because of the inefficient energy sink involved in livestock production. Beef is the single largest contributor for every internal climate and pollutant drivers associated to land use and its residual atmospheric forcings. The modern food supply chain is not only incredibility resource intensive but also threatens human health by introducing dangerous levels of carcinogens, inorganic compounds, micro plastics, microbial organisms, and ionizing radiation into the average diet. Animal agriculture has been investigated for its contribution to the climate crisis and subsequent anthromes (anthropogenic biomes) generated from biogeophysical changes in land cover, freshwater withdrawals, acidification, eutrophication and GHG emissions. The culmination of the cascading effects caused by Concentrated Animal Feeding Operations (CAFOs) jeopardize agricultural Critical Loads (quantitative estimates of the thresholds below which the exposure to a pollutant is not predicted to cause long term statistically significant adverse effects). As these thresholds approach maximum capacity water and food shortages become exponentially more threatening ultimately shifting the classification of these resources from renewable to finite. On this global scale, the continued exploitation of natural ecosystems is not projected to sustain current population trends without drastic mitigation towards conservation.

Nynaeve Phillipson

Impact of mantle structure on True Polar Wander predicted from mantle convection

True Polar Wander (TPW) is the motion of the solid Earth as a whole with respect to the rotation axis. TPW may be produced by large scale mass redistributions, either on the Earth's surface or within the mantle, that perturb the Earth's moment of inertia. One large scale mechanism that can change the distribution of mass within the mantle is the process of mantle convection. Geodynamic retrodictions that assimilate reconstructions of past plate motions can calculate, explicitly, past mantle states and use them to predict TPW back in time. However, such predictions are subject to a number of geological and geodynamic assumptions, such as the distribution of past subduction zones and the viscosity of the Earth's mantle. A comparison of the geodynamically-modeled TPW against paleomagnetic estimates can thus help discriminate competing assumptions. Here we compare TPW histories estimated from two global plate tectonic reconstructions that were assimilated into the TERRA mantle convection code: (1) the widely used Earthbyte 'corrected R' global plate model (Matthews et al., 2016); and (2) TOMOPAC-22, a newly developed global plate tectonic model of the circum-Pacific using structurally restored slabs from mantle seismic tomography (Wu et al., 2022). We discuss the mechanisms that drive the widely varying predictions between models by mapping slabs at target depths indicated by radial power spectra. Any change in mantle structure at these depths will have the greatest impact on predicted TPW.

Student Committee

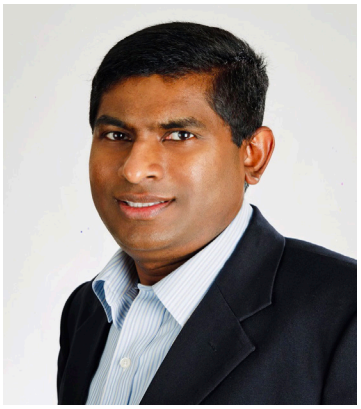

Thishan Karandana
Conference Chair

I am a first-year PhD student in Atmospheric Sciences. I am working on a combination of air quality, forest fires, meteorology, and satellite measurements under the supervision of Prof. Xun Jiang. I received my BS from Sri Lanka in Physics, and the research I did on air quality motivated me towards graduate studies. Being a nature lover, findings from the research that I plan on doing would lead to better control of some of the global threats that we are facing today.

Tabitha Lee
Conference Co-chair

I am a third-year Ph.D. student in atmospheric science working under the advisory of Dr. Yuxuan Wang. Previously, I earned my B.S. in environmental sciences with a concentration in atmospheric sciences at the University of Houston. My work concerns identifying and quantifying unreported NO_2 hotspots in satellite datasets. I hope my work can increase the societal benefit of satellite observations and allow for overlooked or remote locations to have their air quality assessed

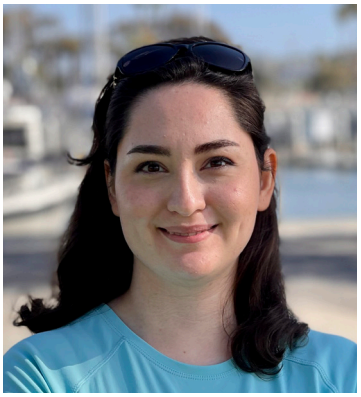

Mahsa Payami
Logistics and Content Creator

I am a first-year PhD student in Atmospheric Sciences. I am doing my research under the supervision of Dr. Choi on AI applications in air quality modeling. My academic journey began with a BSc in Civil Engineering, followed by an MSc in Environmental Engineering. Outside of academia, I have a passion for both painting, hiking, and experiencing new cultures through traveling, which I pursue during my leisure time.

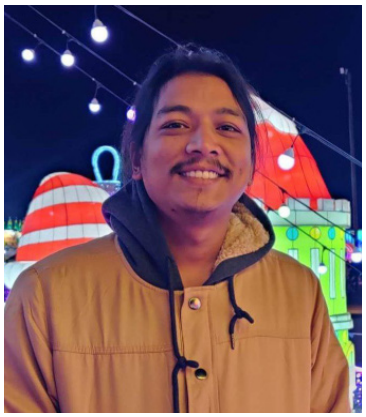

Sagun Gopal Kayastha

Logistics and Content Creator

I'm a first-year PhD student working with Dr. Yunsoo Choi, and my research focuses on exploring the applications of Machine Learning and Artificial Intelligence in the Earth and Atmospheric Science domain. My background is in Environmental Engineering, and I completed my B. Tech at Kathmandu University, Nepal. Prior to starting my PhD, I worked as a Machine Learning Developer at Inspiring Labs Nepal. Aside from my research work, I enjoy programming and learning new skills.

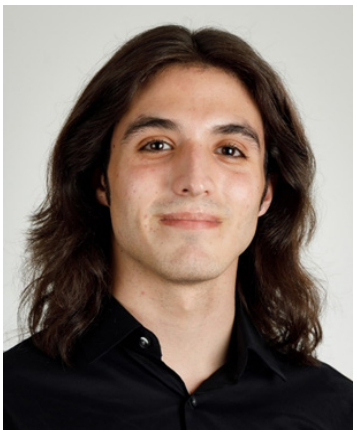

Steven Ramirez

NSMIT Liaison

I am a geology major with a minor in geophysics currently in my last semester of undergraduate. I previously worked under Dr. Jonny Wu conducting plate reconstruction modeling and mapping within the Pacific basin. Starting Fall 2023, I will be attending Brown University to work on my PhD in Planetary Sciences under the direction of Dr. Alexander Evans.

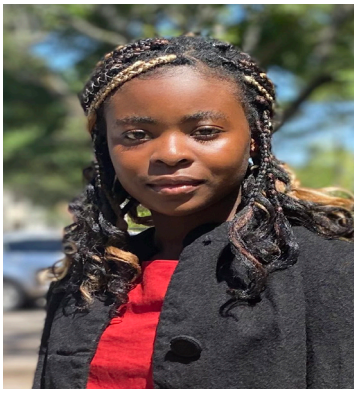

Linda Kitonge

Oral & Poster Sessions Host

I am a second-year undergraduate student in the Department of Earth and Atmospheric Sciences. I am pursuing a B.S. in Environmental Sciences with a concentration in Geosciences at the University of Houston. My interest in Earth Science stems from my curiosity to learn about the Earth and its habitable environments and how humans have affected it over the years. I do hope the knowledge that I will gain here can be helpful in informing society about the physical world and the environment in which we live and how it can be preserved.

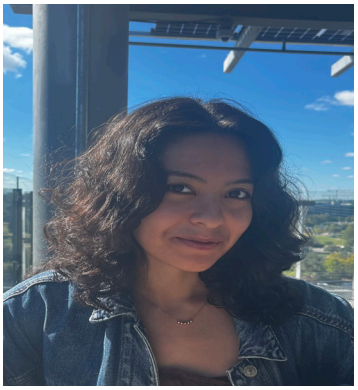

Alina Salinas

Oral & Poster Sessions Host

I am a freshman undergraduate student in the Environmental Science - Geosciences major. My main interests are in geology and soil sciences. My goal is to research geochemical cycles as they pertain to soil formation and the role they play in the earth's microbiome. I also plan to work toward a Biology double major and a minor in energy and sustainability. I am also a part of the UH Honors College and enjoy being outdoors in my free time.

We would like to thank all who volunteered as judges for this event, whether from EAS faculty and staff, industry guests, University of Houston Alumni, or some combination therein. The Student Research Conference would not be what it is without you!

Zheng, Yingcai

Sager, William

Beverly, Emily

Copeland, Peter

Richardson, Mark

Choi, Yunsoo

Jiang, Xun

McLin, Kristie

Castillo, Fernando

Rappenglueck, Bernhard

Wellner, Julia

Stewart, Robert

Zhang, Honghai

Wright, Shawn

Carlson, Brandee

Koster, Klaas

Wang, Ye

Sisson, Jinny

Chinaemerem, Kanu

Sanja, Knezevic Antonijevic

We would also like to thank and acknowledge the College of Natural Science and Mathematics for their contributions to the 2023 Student Research Conference. Thank you for your support

UNIVERSITY OF HOUSTON

COLLEGE OF NATURAL SCIENCE AND MATHEMATICS

WHO ARE WE?

The Department of Earth and Atmospheric Sciences at the University of Houston has a wide range of research programs central to the earth sciences.

- Air Pollution
- Air Quality
- Applied Geophysics
- Applied Rock Physics
- Atmospheric Science
- Carbonate Petrology
- Climatology
- Geodynamics
- GIS
- Hydrology
- Igneous Petrology
- Inorganic Geochemistry
- Isotope Geochemistry
- Marine Geology
- Micropaleontology
- Potential Fields
- Remote Sensing
- Sedimentology
- Seismology
- Sequence Stratigraphy
- Structural Geology
- Tectonics
- Thermochronology
- Whole Earth Geophysics

The Department offers M.S. and Ph.D. degrees in Geology, Geophysics, and Atmospheric Sciences, a B.S. in Geology, Geophysics, and Environmental Sciences, and a B.A. in Earth Sciences. Fieldwork is a major component of all degree programs. The Department also offers Professional M.S. programs in Petroleum Geology and Petroleum Geophysics that are offered at convenient hours for professional geoscientists working in industry or aspiring for a professional position within the petroleum industry.

CONTACT US

Department of Earth and Atmospheric Sciences
4800 Cullen Boulevard, Houston, TX 77204
(713) 743-3399
http://www.eas.uh.edu